Submitted version on Author's Personal Website: C. R. Koch

Article Name with DOI link to Final Published Version complete citation:

M. Shahbakhti, A. Ghazimirsaied, and C. R. Koch. Modeling ranges of cyclic variability for HCCI ignition timing control. In *Proceedings of the ASME 2011 Dynamic Systems and Control Conference*, page 8, Nov 2011

See also:

https://sites.ualberta.ca/~ckoch/open_access/DSCC_2011.pdf

Pre-print

As per publisher copyright is ©2011

This work is licensed under a
Creative Commons Attribution-NonCommercial-NoDerivatives 4.0 International License.

Article submitted version starts on the next page ⟶

Or link: to Author's Website

MODELING RANGES OF CYCLIC VARIABILITY FOR HCCI IGNITION TIMING CONTROL

Mahdi Shahbakhti*
Department of Mechanical Engineering
University of California
Berkeley, California 94720-1740
Email: M.Shahbakhti@berkeley.edu

Ahmad Ghazimirsaied, Charles Robert Koch
Department of Mechanical Engineering
University of Alberta
Edmonton, Alberta T6G 2G8, Canada

ABSTRACT

The probability distribution shape of the ignition timing ensemble allows detection of unstable operation near misfire in Homogeneous Charge Compression Ignition (HCCI) engines. The acceptable range of cyclic variation in HCCI combustion timing is determined by linking the experimental measurements with the shape factors of Generalized Extreme Value (GEV) probability distribution. A combined physical-statistical model is incorporated to analyze the range of cyclic variability in CA50 (crank angle of 50% mass fraction fuel burnt) for two single-cylinder engines. The model is validated with the experimental data at 227 operating points with five different Primary Reference Fuels (PRF). Good agreement between simulation and the experiment with an average error of 0.36 crank angle degree for predicting standard deviation of CA50 is obtained. Low, medium and high cyclic variability zones are identified as a function of intake manifold pressure, equivalence ratio, and intake manifold temperature. This information can be integrated into the design of an engine controller strategy to maintain acceptable levels of cyclic variation during a commanded engine load change.

NOMENCLATURE

aTDC	after Top Dead Center
CAD	Crank Angle Degree
CA50	Crank Angle for 50% burnt fuel
EGR	Exhaust Gas Recirculation
EVC/O	Exhaust Valve Closing/Opening
GEV	Generalized Extreme Value
HCCI	Homogeneous Charge Compression Ignition
IVC/O	Intake Valve Closing/Opening
MKIM	Modified Knock Integral Model
PRF	Primary Reference Fuels
SOC	Start of Combustion
STD	Standard Deviation

*Address all correspondence to this author.

INTRODUCTION

In the past decade, HCCI engines have captured a lot of attention as a promising future engine technology since they have negligible NOx and soot emissions with a thermal efficiency as high as 48% [1]. Fuel saving gains up to 30% compared to conventional engines has made HCCI very attractive for car manufacturers. Some of major car manufacturers (e.g. GM, VW, Mercedes-Benz, and Honda) have already built functioning prototype HCCI engines but stability and control of the HCCI combustion process continues to be the major barriers to commercial implementation.

Control of HCCI ignition timing, particularly for a wide load and speed range, is recognized as the most challenging problem in HCCI engines [2]. Sensitivity to charge initial conditions and the lack of a direct method to initiate ignition make it difficult to control cyclic variations of HCCI ignition timing. Boundaries of high cyclic variations limit HCCI high and low load operation ranges. Results in [1, 3] show that a desirable high-load HCCI operation can be obtained only by using highly retarded ignition timing that occurs early in the expansion stroke. Undesirable cyclic variation of ignition timing increases for these late ignitions which limits the load range of the high efficiency HCCI combustion. For the high cyclic variation regions understanding the characteristics of cyclic variations is a crucial first step in order to control and stabilize them in future HCCI engines.

Cyclic variations in HCCI engines have been investigated in a number of studies [3,4,5,6,7]. The majority of these studies concentrate on cyclic variations of mean effective pressure, engine emissions and pressure related parameters such as peak pressure rise rate. Only a few of these studies [3,4] focus on understanding cyclic variations of ignition timing in HCCI engines. To our knowledge, only in [8] has the distribution shape of ignition timing (CA50) been investigated for an HCCI engine. The results indicate that cyclic variation of HCCI ignition timing seems to display different patterns depending on the physics occurring inside the cylinder. The three most common patterns are shown using normal probability plots in Figure 1. Each plot in Figure 1 shows the normal probability of 200 consecutive engine cycles at one steady-state operating point. The patterns can be categorized as straight,

Copyright © by ASME

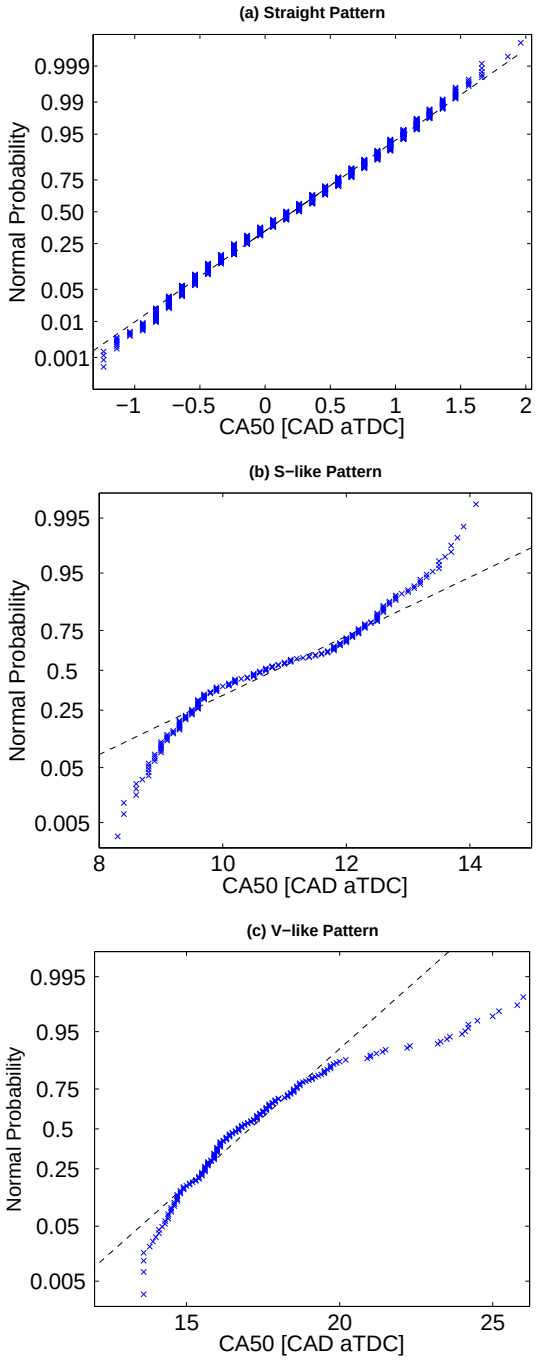

Figure 1. TYPICAL NORMAL PROBABILITY PATTERNS. (a) PRF0, N=1000rpm, Φ= 0.33, EGR=0%, P_m=132 kPa, T_m=134°C; (b) PRF0, N = 800 rpm, Φ= 0.44, EGR= 0 %, P_m= 120 kPa, T_m= 50 °C; (c) PRF10, N= 1000 rpm, Φ= 0.46, EGR= 0 %, P_m= 109 kPa, T_m= 71 °C.

S-like, and V-like. Figure 1(a) represents a knocking operating point which has low cyclic variation with ignitions occurring early (CA50$\approx$ 0.5 *CAD aTDC*). The operating point in Figure 1(b) is typical of a late ignition with high cyclic variation. Normal HCCI operating points with low cyclic variation also show S-like pattern but their marked departure from the straight line at the tails of the data is smaller. The third operating point in Figure 1(c) is an example of late ignition with very high cyclic variations (mean CA50 = 17.5 CAD aTDC, range of ignition timing = 13 CAD). Engine operating points close to knock limit usually show the minimum deviation from the straight line in the normal probability plot, while the majority of the other points particularly those with high cyclic variability have either a S-like pattern or a V-like pattern as shown in Figure 1. Assuming a normal distribution for the random component of the data, deviations from a normal distribution indicate a deterministic component in the data [9]. This suggests more deterministic patterns in the data that has a high deviation from a straight line. Chaotic methods, used in [10] to characterize CA50 ensembles, confirm that there are deterministic patterns near the misfire limit where cyclic variability is the highest.

In this work, the distribution shapes of ignition timing ensemble are linked to the ranges of cyclic variability. The limits of high and low ignition cyclic variation are determined for two different engines at a range of operating conditions. The influence of intake pressure, equivalence ratio, and intake temperature on cyclic variability limits is discussed. The experimental data is used to parameterize a model and then the model is validated using other experimental data to extend [8]. CA50 is selected as the most suitable parameter for future HCCI combustion control [11].

This paper is organized as follows. The first section describes the engine setup used to collect the experimental data. Next, a probability distribution model for CA50 ensemble is explained and the shape factors from the model are linked to the limits of cyclic variability. Then, the model is experimentally validated over a range of operating conditions. Finally, the model is used to calculate the ranges of cyclic variability for the two engines as engine parameters are varied.

EXPERIMENTAL SETUP

Steady-state experimental measurements based on two single-cylinder engines are recorded. The two engines consist of Ricardo Hydra Mark III base fitted with either a Rover K7 cylinder head or a Mercedes E550 camshaft phasing cylinder head. Table 1 specifies the geometry of the two engines. Both engines have a combustion chamber with pent-roof design with a centrally located spark plug and a cast aluminium piston with valve reliefs. Dual camshafts located in the cylinder head operate two intake and two exhaust valves. More details about the design of these two engines are found in [12, 13].

A schematic diagram of the experimental setup is shown in Figure 2. Two separate fuel systems with a fuel pressure of 3 bar are used with the injection timing set to ensure injection occurs only when the intake valves are closed. One of the fuel systems is used to inject n-Heptane and the other is used to inject iso-Octane. A dSpace MicroAutobox 1401/1501 ECU is used to control the injection pulse width of n-Heptane and iso-Octane injectors to provide the desired equivalence ratio and octane number. Two Bosch fuel injectors (model 0-0280-155-844) with a nominal flow rate of 8.2 kg/hr at 310 kPa are used. Although injector pulse widths are maintained constant for each experiment, variations in flow rate are likely due to changes in fuel pressure, and fuel injectors' supplied voltage which comes from a voltage controlled power supply. A maximum variability of 2.8% is estimated for iso-octane and n-

[1]Both engines operate at a constant valve timing with opening/closing point defined at the valve lift of 0.15 mm [14].

Copyright © by ASME

Table 1. CONFIGURATION OF THE TWO SINGLE-CYLINDER ENGINES USED IN THIS STUDY. (IVO: INTAKE VALVE OPENING, IVC: INTAKE VALVE CLOSING, EVO: EXHAUST VALVE OPENING, EVC: EXHAUST VALVE CLOSING, aBDC: AFTER BOTTOM DEAD CENTER)

Parameters	**Mercedes**	**Rover**
Bore × Stroke [mm]	97 × 88.9	80 × 88.9
Compression Ratio	12	10
Displacement [L]	0.657	0.447
Number of Valves	4	4
IVO, IVC[1] [aBDC]	−170°, 40°	−175°, 55°
EVO, EVC [aBDC]	−62°, 148°	−70°, −175°

heptane flow rates [12].

The fresh intake air entering the engine first passes through a laminar airflow meter for flowrate measurement. Then, the fresh charge is mixed with recirculated hot exhaust gases using an insulated return line from the exhaust to the intake manifold. Next, a supercharger driven by a variable speed electric motor adjusts the intake manifold pressure and then a 600W electrical band-type heater sets the mixture temperature to the desired value using a closed-loop controller. To calculate equivalence ratio (Φ), the engine-out air

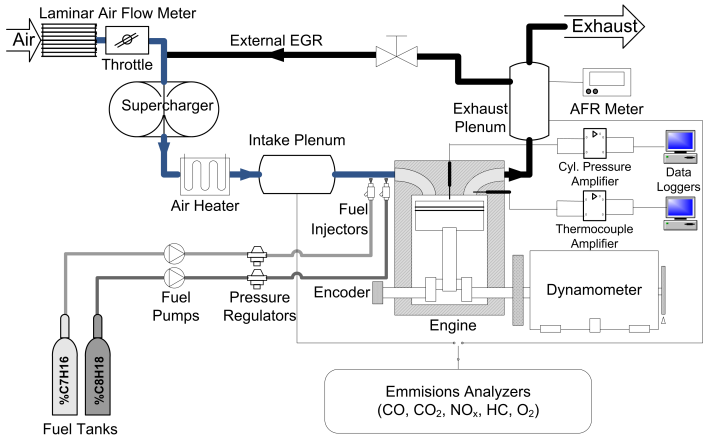

Figure 2. RICARDO SINGLE CYLINDER TESTBENCH SCHEMATIC

fuel ratio is measured with an ECM AFRecorder 1200 universal exhaust gas oxygen sensor. The intake temperature is measured using a K-type thermocouple positioned in the intake manifold. Measurement of the cylinder pressure is made using a Kistler watercooled ThermoCOMP (model 6043A60) piezoelectric pressure sensor that is flush mounted in the cylinder head. The EGR rate is determined by comparing the CO_2 concentrations in the intake and exhaust manifolds, and by assuming that all CO_2 in the intake manifold is from the exhaust gases.

To parameterize each engine model, steady-state (all inputs are held constant) experimental points are run. Table 2 details the experimental conditions of the 227 steady-state points used in this study. The relatively low compression ratios of the engines result in HCCI operation occurring only for lower octane number fuels (PRF equals octane number) and at lower engine speeds. PRF= 40 (PRF40) for these two engines is the highest PRF for which HCCI operation is possible for a range of loads.

Table 2. STEADY-STATE ENGINE OPERATING CONDITIONS FOR THE ROVER HEAD ENGINE (203 POINTS) AND THE MERCEDES HEAD ENGINE (24 POINTS).

Variables	**Mercedes**	**Rover**
Fuel (PRF[2])	0, 10, 20, 30, 40	0, 10, 20, 40
N [rpm]	1000	800, 1000
T_{man} [°C]	80 - 81	41 - 152
EGR [%]	0	0 - 28.5
Φ	0.34 - 0.54	0.29 - 0.94
P_{man} [kPa]	91 - 121	89 - 145
$T_{coolant}$ / T_{oil} [°C]	57 - 80	61 - 83

The engine variables in Table 2 are measured at a constant sample rate of 100 Hz. Cylinder pressure is measured at 0.1 CAD for 200 consecutive engine cycles. The cylinder pressure is then filtered off-line by using a second order Butterworth low pass filter with cutoff frequency of $f_c = 0.556\text{CAD}^{-1}$. Fuel mass fraction burnt parameters such as CA50 are calculated by applying Rassweiler method to the cylinder pressure trace. The mean of CA50 is calculated for 200 cycles at each test point and the cyclic variability of CA50 is characterized by Standard Deviation (STD) which is a common measure of cyclic variability for crank angle based parameters like CA50 [15, 16].

PROBABILITY DISTRIBUTION MODEL

Deterministic patterns in ignition timing ensembles increase substantially as the operating point nears either partial burn or misfire operation and the cyclic variability of combustion increases [10]. A change in the shape of ignition timing ensembles for the engine operation at knocking (low cyclic variability operation) compared to that at misfiring (high cyclic variability operation) is observed. This can be seen in the normal probability plot changing from a straight pattern to S-like or V-like patterns. The Generalized Extreme Value (GEV) distribution is found [8] to cover the range of distribution shapes observed for CA50 ensembles. GEV is a continuous range of shapes by combining three simpler distributions into a single form and the probability density function for the GEV distribution is given by [17]:

$$P(x) = \begin{cases} \frac{1}{\sigma} exp\left[-\left[1-k\frac{(x-\mu)}{\sigma}\right]^{\frac{1}{k}}\right]\left[1-k\frac{(x-\mu)}{\sigma}\right]^{\frac{1}{k-1}} & (a) \\ \\ \frac{1}{\sigma} exp\left[-exp\left(\frac{\mu-x}{\sigma}\right)\right] exp\left(\frac{\mu-x}{\sigma}\right), \quad k=0 & (b) \end{cases} \tag{1}$$

[2]PRF number is defined as the volume percentage of iso-Octane in fuel mixture of n-Heptane and iso-Octane.

Copyright © by ASME

where μ is a location parameter σ is a scale parameter and k is a shape parameter. For each steady-state operating point in Table 2 200 CA50 values are calculated and μ is taken to be the mean of CA50 and σ the STD of CA50 ($\sigma_{CA_{50}}$). The mean of CA50 is taken as the location parameter and STD of CA50 is selected as the scale parameter. The shape parameter k is calculated using a maximum likelihood estimator [17] for the GEV distribution given CA50. The shape parameter k is plotted as a function of σ for the experimental data points in Figure 3. A positive value of k is found for the data points with V-like patterns, but a negative value of k is found for the data points with S-like or straight patterns. The V-like pattern data points have the highest cyclic variability and they are found to be close to partial burn/misfire operation. They exhibit patterns in which a weak partial burn cycle is followed by a strong cycle. This coupling between consecutive ignition timings causes deterministic structure that is reflected as a V-like pattern in a normal probability plot. All of the engine operating points with V-like patterns in Figure 3 have $\sigma_{CA_{50}} \geq 2.6\ CAD$. Thus a limit of $\sigma_{CA_{50}} = 2.6\ CAD$ is used as the threshold to determine if the engine is approaching the high cyclic variability region. Further increase will result in misfiring operation.

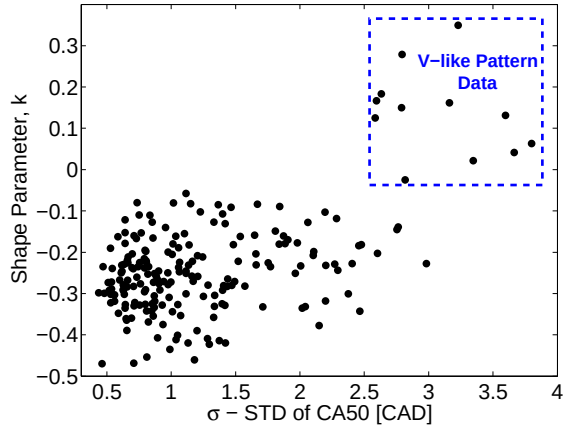

Figure 3. SHAPE PARAMETER k (BY THE GEV MAXIMUM LIKELIHOOD ESTIMATOR [17]) VERSUS σ OF CA50 FOR 203 STEADY-STATE ENGINE CONDITIONS.

EXPERIMENTAL VALIDATION

Estimation of $\sigma_{CA_{50}}$ is necessary for finding the high cyclic variation region discussed above. A model from [8,18] is parameterized to predict $\sigma_{CA_{50}}$ for each of the two engines in Table 1. A description of the model and values of parameters are detailed in the Appendix. Experimental data from the two engines are used to parameterize and validate the model at the 227 operating conditions listed in Table 2.

Predicted CA50 from the model is compared with experimental CA50 results in Figure 4 for all operating conditions. The range of CA50 variation from 200 consecutive cycles for each operating point is also shown in Figure 4. The diamond symbol indicates the average experimental CA50 while the round symbol shows the predicted CA50 from the model. The average error value shown in the figure is the error between experimental (diamond symbols) and predicted (round symbols) values. An average error of 1.39 CAD and 1.15 CAD is observed for Rover engine and Mercedes engine

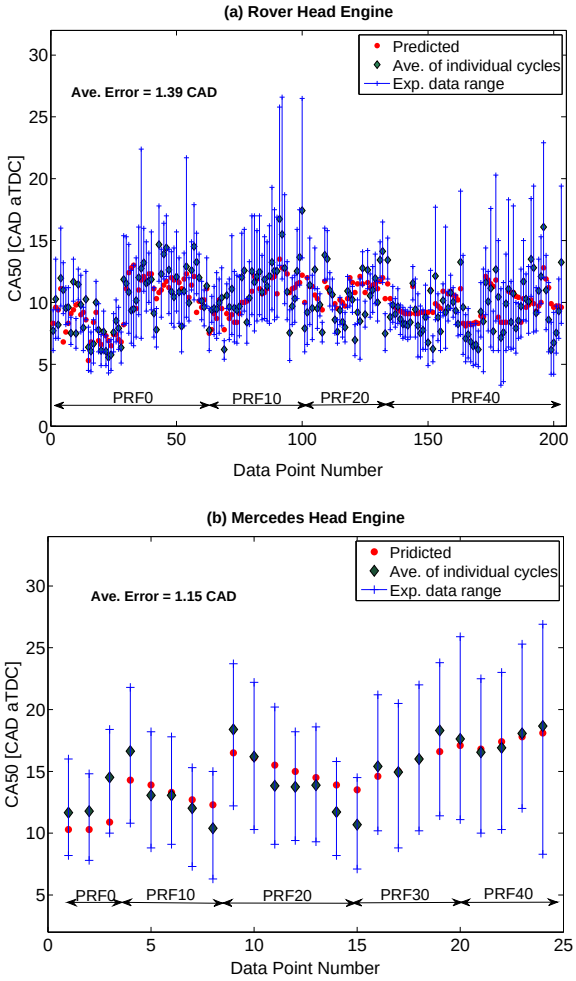

Figure 4. COMPARISON BETWEEN PREDICTED AND EXPERIMENTAL CA50 FOR FIVE PRF BLENDS AT 227 DIFFERENT STEADY-STATE ENGINE CONDITIONS FROM TWO DIFFERENT ENGINES.

respectively. The model predictions usually fall within the CA50 experimental range for the 227 engine operating points tested, indicating the model predicts the CA50 mean accurately for the two engines running with five different octane numbers.

The location of ignition timing (CA50) is a predominant factor on the cyclic variation of CA50 [8]. Ranges of cyclic variation in Figure 4 show a higher cyclic variation of CA50 when CA50 occurs late in the combustion cycle. The predicted CA50 from the model, shown in Figure 4, is one main input needed to the subsequent cyclic variability model used to predict $\sigma_{CA_{50}}$ (details in Appendix). A comparison between predicted $\sigma_{CA_{50}}$ with those of experiments is shown in Figure 5. The total average error for the 227 steady-state operating points in Figure 5 is 0.36 CAD. The prediction accuracy can be improved by incorporating more details into the cyclic variability model. For instance the model ignores the effects from changing the coolant temperature on $\sigma_{CA_{50}}$, but there are coolant temperature differences up to 23°C between operating points in Table 2. Cyclic variation of ignition timing increases by reducing the coolant temperature due to the changes in the cylinder wall thermal boundary layer and also variations in thermal stratification inside the cylinder [4]. A higher cyclic variation is observed in Figure 5 for the Mercedes engine compared to that of the Rover

Copyright © by ASME

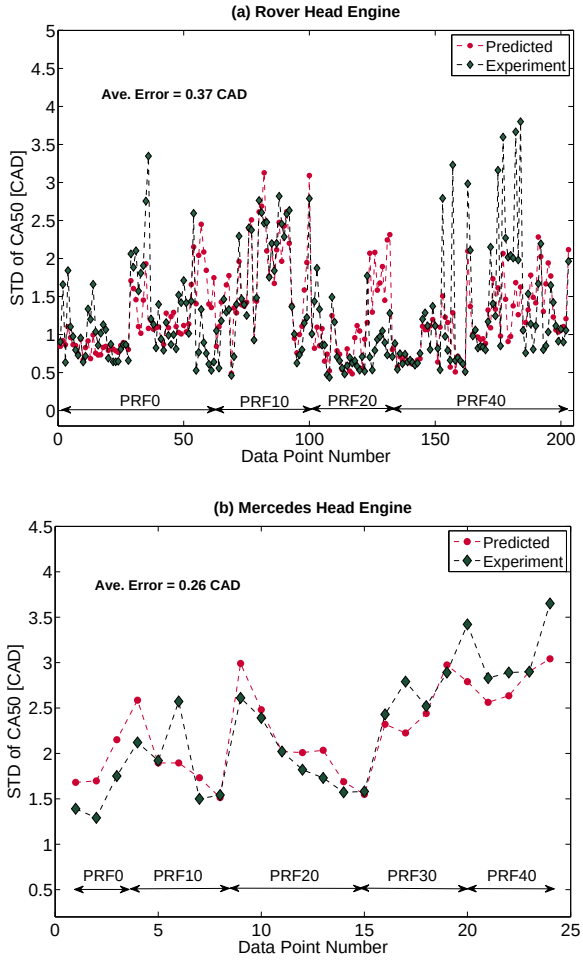

Figure 5. COMPARISON BETWEEN PREDICTED AND EXPERIMENTAL $\sigma_{CA_{50}}$ FOR FIVE PRF BLENDS AT 227 DIFFERENT STEADY-STATE ENGINE CONDITIONS FROM TWO DIFFERENT ENGINES.

engine. This can be explained by comparing the Figure 4(a) and 4(b) where the Mercedes data points generally have more delayed ignitions and higher CA50s.

Predicting Operating Ranges of Cyclic Variation

Calculating HCCI operating ranges corresponding to certain levels of ignition timing cyclic variability is of great utility. This information can be used by the ignition timing controller to avoid unstable and undesirable engine operation. Results of the experimental study in [4, 19] for the Rover and Mercedes engines indicate that $\sigma_{CA_{50}} \leq 1.7$ CAD is the limit for desirable HCCI operation. Below this limit cyclic variation is low and metrics for ignition timing control are correlated. The results from this work indicate $\sigma_{CA_{50}} > 2.6$ CAD leads to V-like high cyclic operation. Thus the following levels of ignition timing cyclic variability operation are defined:

$$\sigma_{CA_{50}} \begin{cases} \leq 1.7\ CAD & \text{low cyclic} \\ 1.7\ CAD < \ \leq\ 2.6\ CAD & \text{intermediate cyclic} \\ > 2.6\ CAD & \text{high cyclic} \end{cases}$$

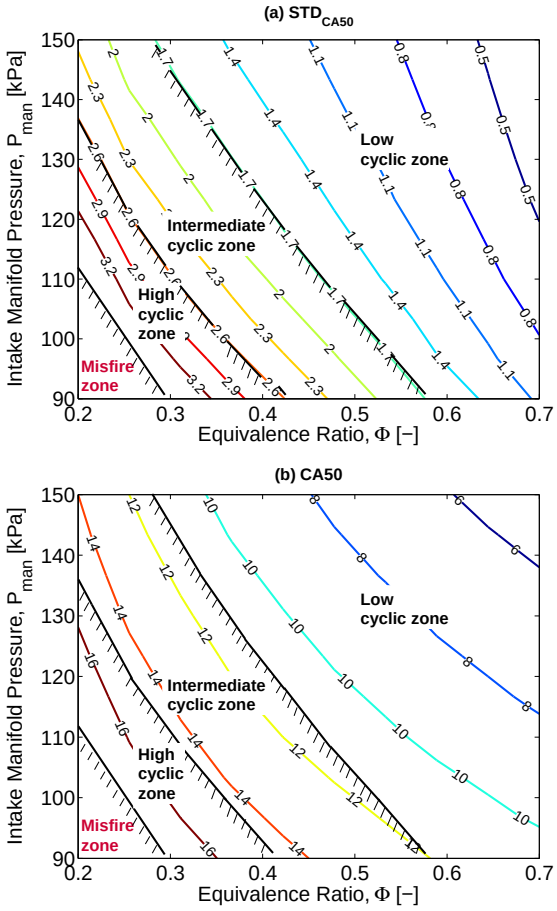

Figure 6. STD$_{CA50}$ AND CA50 FOR HCCI OPERATION OF ROVER ENGINE USING PRF40 FUEL. (N= 1000 rpm, T_m= 80°C, EGR= 0%)

The parameterized model is used to map contours of $\sigma_{CA_{50}}$ and CA50 versus variations of intake manifold pressure (P_{man}) and equivalence ratio (Φ). The results are shown in Figures 6 and 7 for the two engines. The levels defined above are then used to map the low, medium, and high cyclic variability operating zones. A higher cyclic variation of CA50 is observed in Figures 6 and 7 for operating conditions with leaner mixtures at lower intake pressures. This can be partly explained by examining Figure 6(b) and 7(b) where ignition timing (CA50) retards by decreasing either the equivalence ratio or the intake pressure. Higher cyclic variations by retarding ignition timing after TDC (when CA50 increases in Figures 6(b) and 7(b)) is attributed to different factors including counteracting the temperature rise from combustion by the cooling from piston expansion, and higher charge stratifications for late ignitions [4, 20]. Combustion efficiency and thermal efficiency for ultra lean mixtures are low [4, 21]. The low efficiency results in weak combustion in ultra lean conditions and consequently the combustion is more sensitive to any small fluctuations in the intake charge properties. A higher cyclic variation in ignition timing for ultra lean mixtures is observed in Figure 6(a) and Figure 7(a) as expected. The results in Figures 6 and 7 are also consistent with the experimental observations in [4].

The low cyclic variation zone is larger in Figure 6(a) compared to that of Figure 7(a). This is attributed to CA50 being more delayed for the Mercedes engine as evidenced by comparing CA50

Copyright © by ASME

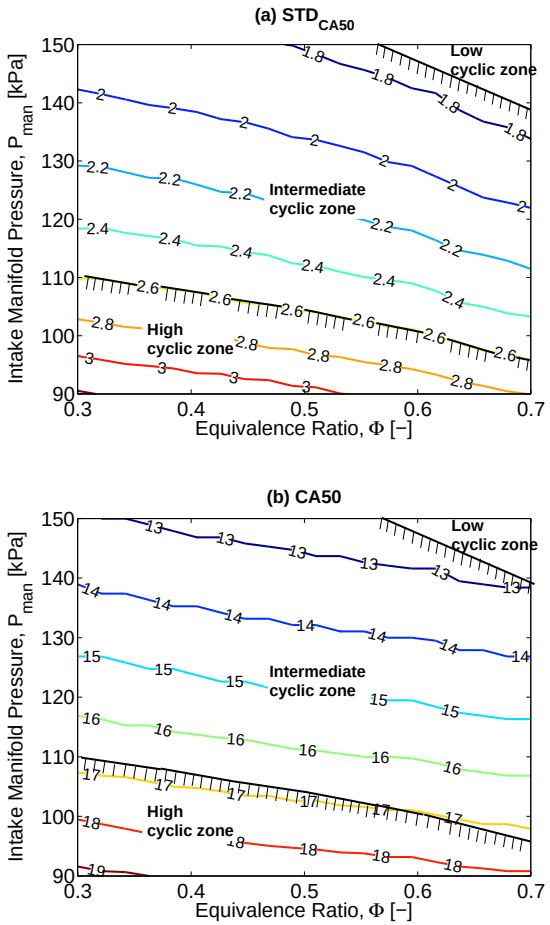

Figure 7. STD$_{CA50}$ AND CA50 FOR HCCI OPERATION OF MERCEDES ENGINE USING PRF40 FUEL. (N= 1000 rpm, T_m= 80°C, EGR= 0%)

in Figure 6(b) with 7(b). This is also observed in the experimental data in Figure 4(b) compared to those in Figure 4(a). The CA50 limit for low and high cyclic variations are also shown in Figures 6 and 7. The CA50 levels for the Rover engine operation are:

$$CA_{50}\begin{cases} \leq 11.5^{\circ}aTDC & \text{low cyclic} \\ 11.5^{\circ}aTDC < \ \leq 15^{\circ}aTDC & \text{intermediate cyclic} \\ > 15^{\circ}aTDC & \text{high cyclic} \end{cases}$$

The limits for the Mercedes engine are higher and the engine has the high cyclic operation when CA50 occurs after 17 CAD aTDC. The higher tolerance to cyclic variability in the Mercedes engine is attributed to a higher compression ratio – as seen in Table 1.

The effect of the intake manifold temperature on low and high cyclic variability limits are shown in Figure 8 for the Rover engine. On the $\Phi - P_{man}$ plane the low cyclic variability zone becomes larger with increasing intake manifold temperatures. This is consistent with the experimental observations in [4, 22] where cyclic variation of the ignition timing reduces by increasing the intake manifold temperature. Higher cyclic variation at lower intake temperatures can be explained by a combination of three main effects. One effect, CA50 increases (retards) after TDC when decreasing the intake temperature. As previously mentioned, a higher level of cyclic

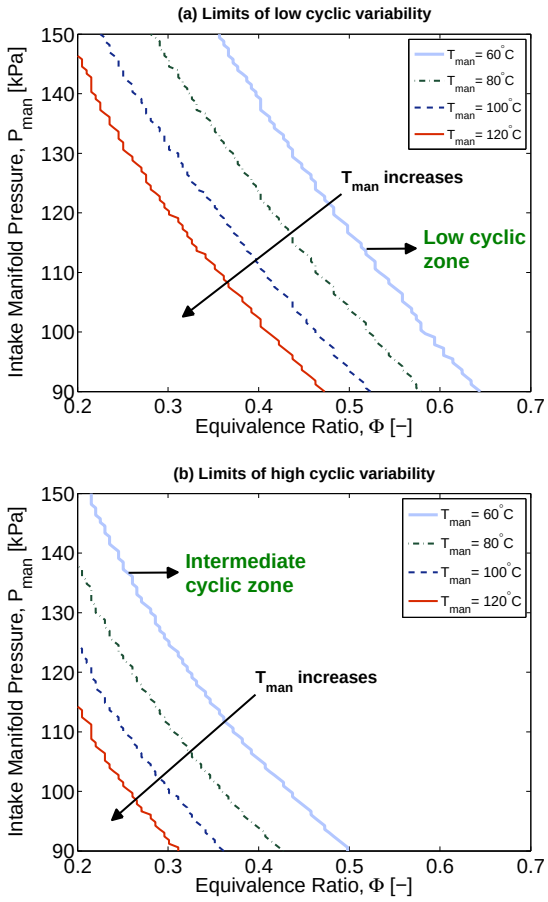

Figure 8. LIMITS FOR LOW AND HIGH CYCLIC VARIABILITY REGIONS FOR ROVER ENGINE AT DIFFERENT INTAKE TEMPERATURES. (PRF40, N= 1000 rpm, EGR= 0%)

variation is expected by delaying the combustion phasing late after TDC. The second effect is that there is always cyclic fluctuation in the residual gas temperature which causes cyclic fluctuations in the auto-ignition process [15]. Similar cyclic variations of residual gas temperature are less significant at higher intake temperatures since gas core temperatures will be higher [4]. The third effect is that random fluctuations of the charge temperature have less impact on ignition timing of hot ignition when the higher temperature-rise rates occur before Start of Combustion (SOC) [3]. Decreasing the intake temperature leads to a decrease in the temperature-rise before SOC and consequently a higher cyclic variation of hot ignition occurs.

The low cyclic variability limits in Figure 8(a) indicate the operating zone where the ignition timing controller can adjust the cyclic variability of the combustion by controlling one ignition timing metric (e.g. CA50). This is because a good correlation exists between the cyclic variations of CA50 with those of SOC, burn duration, the crank angle of peak heat release, and the crank angle of peak in-cylinder pressure when the engine is operating in the low cyclic zone [4]. However, as engine operation moves into the inter-

Copyright © by ASME

mediate cyclic zone, interrelations among cyclic variations of ignition timing metrics become more complex and controlling only one ignition timing metric is not enough to adjust the cyclic variability of combustion [4].

Results in Figure 8 can be used as a guide to help design the engine control algorithm to maintain acceptable levels of cyclic variation. For example when the engine load increases by increasing P_{man} at a constant Φ this is a vertical movement ($\uparrow$) in Figure 8. Then Figure 8 suggests that the engine controller must command a higher intake manifold temperature to maintain an acceptable level of cyclic variation particularly if the jump in P_{man} causes the engine to jump to the high cyclic zone. Another example is the case where fuel is reduced to decrease engine torque at a constant manifold pressure. This effectively reduces Φ at a constant P_{man} and is a horizontal movement ($\leftarrow$) in Figure 8. Results in Figure 8 suggest that the engine controller must command an appropriate higher intake temperature to maintain acceptable cyclic variation levels. These two examples indicate a potential engine control strategy for maintaining HCCI cyclic variability as a function of changing engine variables.

Summary

Unstable HCCI operation near misfire can be identified by the shape of the ignition timing (CA50) probability distribution. Patterns of ignition timing ensemble distribution are connected with the shape factors of the GEV probability distribution. Data points with V-like patterns are found to have a positive shape factor and they exhibit the highest cyclic variation of CA50. These points with a V-like pattern represent the conditions as the engine approaches unstable HCCI operation. $\sigma_{CA_{50}} \leq 2.6\ CAD$ is found as the limit of high cyclic variability operation for the engine conditions tested.

A physical-empirical model to predict $\sigma_{CA_{50}}$ for two single-cylinder engines is described. Validating the model with 227 steady-state operating points shows good agreement with experiments for the five different PRF fuels tested. A total average error of 1.36 CAD is observed for predicting mean CA50 and an average error of 0.36 CAD is found from comparing the calculated $\sigma_{CA_{50}}$ with the experimental standard deviations.

A range of intake manifold pressures, equivalence ratios and intake manifold temperatures are simulated to predict HCCI combustion cyclic variation. This provides insight into the design of engine control algorithms that respond to command load changes but maintain acceptable levels of cyclic variation. A larger zone of low cyclic variability is found for the two engines when increasing the intake temperature, the equivalence ratio, or the intake pressure. The most stable operating region is found to be where CA50 $\leq$ 13 CAD aTDC and further retarding the ignition timing for 3-4 CAD (CA50 $>$ 17 CAD aTDC) causes the engines to have high cyclic variation operation.

ACKNOWLEDGMENT

The authors gratefully acknowledge the Natural Sciences and Engineering Research Council of Canada (NSERC), and AUTO21 Network of Centers of Excellence for supporting this work.

REFERENCES

[1] Dec, J. E., and *et al.*, 2010. "HCCI and Stratified-Charge CI Engine Combustion". *US DOE annual merit review report*.

[2] Lu, X., and *et al.*, 2005. "Study on the Ignition, Combustion and Emissions of HCCI Combustion Engines Fueled With Primary Reference Fuels". *SAE Paper No. 2005-01-0155*.

[3] Sjöberg, M., and Dec, J. E., 2007. "Comparing Late-Cycle Autoignition Stability for Single- and Two-Stage Ignition Fuels in HCCI Engines". *Proceedings of the Combustion Institute,* **31**, pp. 2895–2902.

[4] Shahbakhti, M., and Koch, C. R., 2008. "Characterizing the Cyclic Variability of Ignition Timing in an HCCI Engine Fueled with n-Heptane/iso-Octane Blend Fuels". *International Journal of Engine Research,* **9**, pp. 361–397.

[5] Li, H. L., and *et al.*, 2007. "Cycle-to-Cycle Variation of a HCCI Engine Operated with n-Heptane". *Proc. of CI/CS Conference*.

[6] Xingcai, L., and *et al.*, 2007. "Experimental Study on the Cycle-by-Cycle Variations of Homogeneous Charge Compression Ignition Combustion Using Primary Reference Fuels and Their Mixtures". *Proc. of IMechE - Part D,* **221**.

[7] Kalghatgi, G. T., and Head, R. A., 2006. "Combustion Limits and Efficiency in a Homogeneous Charge Compression Ignition Engine". *Int. J. of Engine Research,* **7**, pp. 215–236.

[8] Shahbakhti, M., and *et al.*, 2009. "Predicting the Distribution of Combustion Timing Ensemble in an HCCI Engine". *Proc. of ASME- ICES Conference*.

[9] NIST/SEMATECH e-Handbook of Statistical Methods, http://www.itl.nist.gov/div898/handbook/, Jan., 2008.

[10] Ghazimirsaied, A., and *et al.*, 2010. "HCCI Combustion Phasing Prediction Using a Symbol-Statistic Approach". *J. of Engineering for Gas Turbine and Power, Volume 132, Issue 8*.

[11] Bengtsson, J., and *et al.*, 2006. "Hybrid Control of Homogeneous Charge Compression Ignition (HCCI) Engine Dynamics". *Int. J. of Control,* **79**, pp. 422–448.

[12] Lupul, R., 2008. "Steady State and Transient Characterization of a HCCI Engine with Varying Octane Fuel". M.Sc. thesis, University of Alberta.

[13] Audet, A., 2008. "Closed Loop Control of HCCI Using Camshaft Phasing and Dual Fuels". M.Sc. thesis, University of Alberta.

[14] Heywood, J. B., 1988. *Internal Combustion Engine Fundamentals*. McGraw-Hill.

[15] Sjöberg, M., and *et al.*, 2004. "Comparing Enhanced Natural Thermal Stratification Against Retarded Combustion Phasing for Smoothing of HCCI Heat-Release Rates". *SAE Paper No. 2004-01-2994*.

[16] Kumano, K., and Iida, N., 2004. "Analysis of the Effect of Charge Inhomogeneity on HCCI Combustion by Chemiluminescence Measurement". *SAE Paper No. 2004-01-1902*.

[17] Castillo, E., and *et al.*, 2005. *Extreme Value and Related Models with Applications in Engineering and Science*. John Wiley & Sons Publication.

[18] Shahbakhti, M., and Koch, C. R., 2010. "Physics Based Control Oriented Model for HCCI Combustion Timing". *J. of Dynamic Systems, Measurement and Control, Vol. 132*.

[19] Ghazimirsaied, A., and *et al.*, 2011. "Ignition Timing Criteria for Partial Burn Operation in an HCCI Engine". *Proc. of CI/CS Conference*.

[20] Sjöberg, M., and *et al.*, 2005. "Potential of Thermal Stratification and Combustion Retard for Reducing Pressure-Rise

Copyright © by ASME

Rates in HCCI Engines, Based on Multi-Zone Modelling and Experiments". *SAE Paper No. 2005-01-0113*.
[21] Iverson, R. J., and *et al.*, 2005. " The Effects of Intake Charge Preheating in a Gasoline-Fueled HCCI Engine". *SAE Paper No. 2005-01-3742*.
[22] Shahbakhti, M., and *et al.*, 2007. "Cyclic Variations of Ignition Timing in an HCCI Engine". *Proc. of ASME - ICES Conference*.
[23] Kirchen, P., and *et al.*, 2007. "A Skeletal Kinetic Mechanism for PRF Combustion in HCCI Engines". *J. of Combustion Science and Technology,* **179**, pp. 1059–1083.

APPENDIX: IGNITION TIMING DISPERSION MODEL

Mean value and dispersion magnitude of HCCI ignition timing ensemble are predicted using a physical-imperial control-oriented model of HCCI combustion. Inputs of the model are intake pressure, intake temperature, EGR rate, equivalence ratio and engine speed. Using these inputs, the model's outputs are CA50 and STD of CA50. Details of the model and values of the parameters for the Rover engine are found in [8, 18]. Here, a brief description of the model and values of the parameters for the new Mercedes engine are explained. The experimental data listed in Table 2 is used to find parameters of empirical correlations using Nelder-Mead simplex minimization method.

Combustion Model

A physical control-oriented model is used to simulate an HCCI cycle from the intake stroke to the combustion stroke. The main output of this model is CA50 crank angle. Here, the governing equations of the model are described, but the procedure to parameterize the model is found in [18].

IVC temperature & pressure correlation – Semi empirical correlations are used for the intake process to estimate the pressure and temperature of the mixture at Intake Valve Closing (IVC) from the measured values of the intake manifold. IVC pressure is predicted using a correlation from a previous study [18]:

$$P_{ivc} = \frac{N^{A_P} \,.\, \Phi^{B_P}}{T_m^{C_P}} P_m \tag{2}$$

where, N is the engine speed in RPM, and P_m and T_m are the gas pressure and temperature in the intake manifold in kiloPascals (kPa) and in Celsius (°C) respectively and Φ is the equivalence ratio. Values of the parameters for Mercedes engine are $A_P = 0.146, B_P = 0.054$, and $C_P = 0.235$.

The temperature of air-fuel mixture at IVC (T_{ivc}) is predicted using the following correlation [18]:

$$T_{ivc} = \left(A_T \; T_m^2 + B_T \; T_m + C_T\right) \frac{\Phi^{D_T} \,.\, N^{E_T}}{(1+EGR)^{F_T}} \tag{3}$$

where A_T, B_T, C_T, D_T, E_T and F_T are constant parameters and their values for the Mercedes engine are A_T=1.774, B_T=2.363, C_T=1.85, D_T=-0.118, E_T=-0.735, and F_T=1.

SOC model – A Modified Knock-Integral Model (MKIM) [18] is used to predict Start of Combustion (SOC):

$$\int_{\theta_{ivc}}^{\theta_{soc}} \frac{\Phi^{B_M}}{A_M \; N \; exp\left(\frac{C_M \left(P_{ivc} \, v_c^{k_c}\right)^{D_M}}{T_{ivc,mod} \, v_c^{k_c-1}}\right)} \, d\theta = 1.0 \tag{4}$$

where, θ and N represent the engine crank angle and the engine speed, B_M, C_M, and D_M are constant parameters. The value of the expression being integrated increases as the point of SOC is approached. A_M and v_c are determined by:

$$v_c(\theta) = \frac{V_{ivc}}{V(\theta)} \;\; , \; A_M = E_1 X_d + E_2 \tag{5}$$

where, E_1 and E_2 are constant parameters and the cylinder volume, $V(\theta)$, is calculated as a function of crank angle using slider crank mechanism [14]. Parameters E_1, E_2, B_M, C_M, and D_M are unknown and need to be determined to be able to use the MKIM to predict SOC. Over 2400 simulations from a detailed HCCI Thermo-Kinetic Model [23] at a range of operating conditions are used to parameterize the MKIM. This procedure is explained in detail in [18].

Fuel burn rate model – A modified Wiebe function [18] is used to predict fuel mass fraction burned (x_b) to calculate CA50:

$$x_b(\theta) = 1 - exp\left(-A_W \left[\frac{\theta - \theta_{soc}}{\theta_d}\right]^{B_W}\right) \tag{6}$$

where, A_W and B_W are constant parameters and θ_{soc} is SOC crank angle and θ_d is the combustion duration determined by:

$$\theta_d = C_W \left(1 + X_d\right)^{D_W} \; \Phi^{E_W} \tag{7}$$

where, C_W, D_W, and E_W are constant parameters. CA50 ($x_b = 0.5$) is the output of the fuel burn rate model and is the final output of the combustion model. Values of the parameters for the Mercedes engine are A_W=4.36, B_W=5.59 C_W=14.25, D_W=0.005, and E_W=-0.009.

Cyclic Variability Model

Cyclic variability of CA50 is characterized by STD and an empirical correlation is used to estimate the STD of CA50 ($\sigma_{CA_{50}}$) [8]:

$$\sigma_{CA_{50}} = A_D + B_D \,.\, CA_{50}^2 \; Ln\left(CA_{50}\right) + C_D \,.\, D_f \; Ln\left(D_f\right) \tag{8}$$
$$where, \; D_f = \frac{\Phi}{1+EGR}$$

D_f represents the dilution factor and A_D, B_D, and C_D are the dispersion parameters which should be determined for each engine speed. Values of the parameters for the Mercedes engine are A_D = 0.560, B_D = -1.186 and C_D = 0.002.

Copyright © by ASME